Monthly Notices of the ROYAL ASTRONOMICAL SOCIETY
MNRAS Advance Access published April 10, 2013
MNRAS (2013) doi:10.1093/mnras/stt402

Astrometric and photometric initial mass functions from the UKIDSS Galactic Clusters Survey – IV. Upper Sco⋆

N. Lodieu[1,2]†

[1] *Instituto de Astrofísica de Canarias (IAC), Vía Láctea s/n, E-38205 La Laguna, Tenerife, Spain*
[2] *Departamento de Astrofísica, Universidad de La Laguna (ULL), E-38205 La Laguna, Tenerife, Spain*

Accepted 2013 March 4. Received 2013 March 4; in original form 2013 January 21

ABSTRACT

We present the results of a proper motion wide-field near-infrared survey of the entire Upper Sco (USco) association (∼160 square degrees) released as part of the United Kingdom Infrared Telescope Infrared Deep Sky (UKIDSS) Galactic Clusters Survey (GCS) Data Release 10 (DR10). We have identified a sample of ∼400 astrometric and photometric member candidates combining proper motions and photometry in five near-infrared passbands and another 286 with *HK* photometry and 2MASS/GCS proper motions. We also provide revised membership for all previously published USco low-mass stars and substellar members based on our selection and identify new candidates, including in regions affected by extinction. We find negligible variability between the two *K*-band epochs, below the 0.06 mag rms level. We estimate an upper limit of 2.2 per cent for wide common proper motions with projected physical separations less than ∼15 000 au. We derive a disc frequency for USco low-mass stars and brown dwarfs between 26 and 37 per cent, in agreement with estimates in IC 348 and σ Ori. We derive the mass function of the association and find it consistent with the (system) mass function of the solar neighbourhood and other clusters surveyed by the GCS in the 0.2–0.03 $M_{\odot}$ mass range. We confirm the possible excess of brown dwarfs in USco.

Key words: methods: observational – techniques: photometric – brown dwarfs – stars: low-mass – stars: luminosity function, mass function – open clusters and associations: individual: Upper Sco.

1 INTRODUCTION

The knowledge of the number of stars and brown dwarfs as a function of mass in open clusters and star-forming regions is important to address the question of the universality of the initial mass function (Salpeter 1955; Miller & Scalo 1979; Scalo 1986; Kroupa 2002; Chabrier 2003; Kroupa et al. 2011). The advent of large optical and near-infrared detectors has shed light on the properties of low-mass stars and substellar objects in a variety of environments and enabled an in-depth study of the mass function well below the hydrogen-burning limit (see the review by Bastian, Covey & Meyer 2010, and references therein). However, many surveys in young regions lack homogeneity in the multiband photometric coverage and accurate proper motions for brown dwarf members, making the interpretation of their mass spectrum sometimes difficult.

The United Kingdom Infrared Telescope (UKIRT) Infrared Deep Sky Survey (UKIDSS; Lawrence et al. 2007)[1] is a deep large-scale infrared survey conducted with the UKIRT Wide Field Camera (WFCAM; Casali et al. 2007) equipped with five infrared filters (*ZYJHK*; Hewett et al. 2006). All data are pipeline-processed at the Cambridge Astronomical Survey Unit (CASU; Irwin et al. 2004, Irwin et al., in preparation),[2] processed and archived in Edinburgh, and later released to the community through the WFCAM Science Archive (WSA; Hambly et al. 2008).[3] One of its components, the Galactic Clusters Survey (hereafter GCS), imaged ∼1000 square degrees homogeneously in 10 star-forming regions and open clusters down to 0.03–0.01 $M_{\odot}$ (depending on the age and distance of each region) to investigate the universality of the initial mass function. In addition to the photometry, the latest releases of the GCS provide proper motions measured from the different epochs, with accuracies of about five per year (mas yr^{-1}).

The Upper Sco (USco) region is part of the nearest OB association with the Sun, Scorpius Centaurus, located at 145 pc (de

⋆ Based on observations made with the United Kingdom Infrared Telescope, operated by the Joint Astronomy Centre on behalf of the UK Particle Physics and Astronomy Research Council.
† E-mail: nlodieu@iac.es

[1] The survey is described at www.ukidss.org
[2] The CASU WFCAM webpage is at http://apm15.ast.cam.ac.uk/wfcam
[3] WSA is accessible at http://surveys.roe.ac.uk/wsa

Bruijne et al. 1997). Its precise age is currently under debate (Song, Zuckerman & Bessell 2012): earlier studies using isochrone fitting and dynamical studies derived an age of 5 ± 2 Myr (Preibisch & Zinnecker 2002) in agreement with deep surveys (Slesnick, Carpenter & Hillenbrand 2006; Lodieu et al. 2008) but recently challenged by Pecaut, Mamajek & Bubar (2012) who quoted 11 ± 2 Myr from a spectroscopic study of F stars at optical wavelengths. The association was targeted at multiple wavelengths, starting off in X rays (Walter et al. 1994; Preibisch et al. 1998; Kunkel 1999), but also astrometrically with *Hipparcos* (de Bruijne et al. 1997; de Zeeuw et al. 1999), and more recently in the optical (Ardila, Martín & Basri 2000; Preibisch, Guenther & Zinnecker 2001; Preibisch & Zinnecker 2002; Martín, Delfosse & Guieu 2004; Slesnick et al. 2006) and in the near-infrared (Lodieu, Hambly & Jameson 2006; Lodieu et al. 2007; Dawson, Scholz & Ray 2011; Lodieu, Dobbie & Hambly 2011b; Dawson et al. 2013). Tens of brown dwarfs have now been confirmed spectroscopically as USco members (Martín et al. 2004, 2010; Lodieu et al. 2006, 2008, 2011b; Slesnick et al. 2006; Slesnick, Hillenbrand & Carpenter 2008; Dawson et al. 2011) and the mass function of this population determined well into the substellar regime (Slesnick et al. 2008; Lodieu et al. 2011b). Three independent studies noticed that USco may harbour an excess of brown dwarfs (Preibisch et al. 2001; Lodieu et al. 2007; Slesnick et al. 2008). Five T-type candidates reported by Lodieu et al. (2011a) have been rejected as astrometric members of the association (Lodieu et al. 2013).

In this paper, we present a photometric and proper motion based study of ∼50 square degrees in USco released as part of the UKIDSS GCS DR10 (2013 January 14) along with a revised analysis of the GCS Science Verification (SV) data (6.7 square degrees). This study is complemented by *HK* imaging and proper motion from the 2MASS/GCS cross-match for the remaining area of the association. Our work improves on previous studies by selecting members based on accurate proper motions provided by the GCS down to masses as low as 0.01 $M_{\odot}$ and identifying candidates in regions previously unstudied and affected by heavy extinction. In Section 2, we present the photometric and astrometric data set employed to extract USco member candidates. In Section 3, we review the list of previously published USco members recovered by our analysis and revise their membership. In Section 4, we identify new stellar and substellar member candidates based on five-band photometry and astrometry. In Section 5 and 6, we investigate the level of *K*-band variability and disc frequency for USco low-mass stars and brown dwarfs, respectively. In Section 7, we derive the cluster luminosity and (system) mass functions and compare it to earlier estimates for this cluster and others, along with that of the field population. This work is in line with our recent studies of the Pleiades (Lodieu, Deacon & Hambly 2012b), α Per (Lodieu et al. 2012a) and Praesepe (Boudreault et al. 2012) clusters.

2 THE SAMPLE

We selected point sources in the full USco region, defined by RA = 230°–252° and declinations between −32° and −16° (Fig. 1). We retrieved the catalogue using a Structured Query Language (SQL) query similar to our earlier studies of the Pleiades (Lodieu et al. 2012b), α Per (Lodieu et al. 2012a) and Praesepe (Boudreault et al. 2012). Briefly, we selected high-quality point sources with *JHK* photometry, allowing for *Z* and *Y* non-detections. The query returned a total number of 2943 321 sources (Fig. 2). We refer to this sample as the '*ZYJHK*-PM' sample throughout the paper. Below we distinguish the region free of extinction and the one affected by reddening although we will show that the same photometric and astrometric criteria can be applied to provide a clean sample of member candidates.

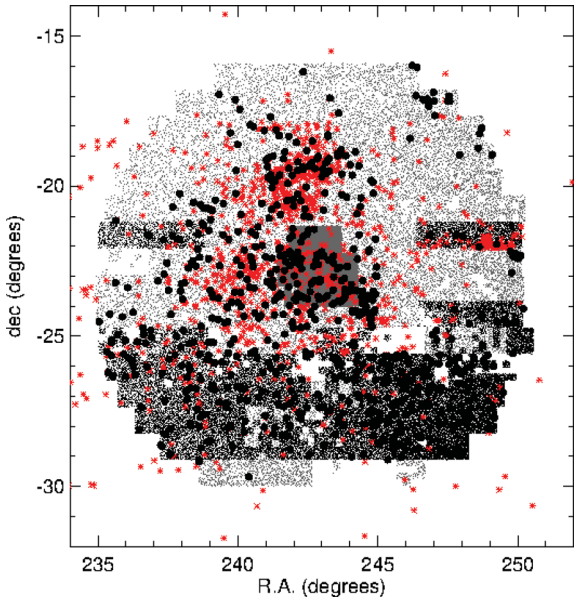

Figure 1. The coverage in USco as released by the UKIDSS GCS DR10: the light grey, dark grey and black patches indicate the *HK*, SV and GCS DR10 samples, respectively. The holes are due to frames removed from the GCS release due to quality control issues. Overplotted are member candidates identified in this work (filled black dots) and previously published sources from the literature (red asterisks).

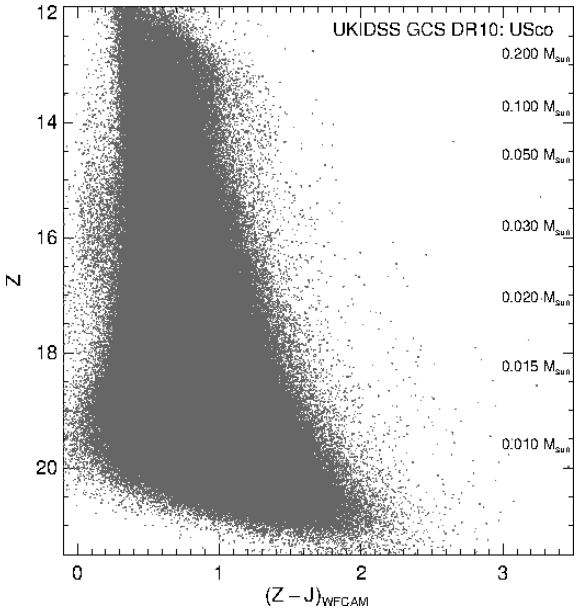

Figure 2. (*Z* − *J*,*Z*) CMD for ∼50 square degrees in USco extracted from the UKIDSS GCS DR10. The mass scale shown on the right-hand side spans ∼0.2–0.08 $M_{\odot}$, following the 5 Myr BT-Settl isochrones (Allard, Homeier & Freytag 2012).

Proper motion measurements are available in the WSA for UKIDSS data releases from DR9 for all the wide/shallow surveys with multiple epoch coverage in each field [i.e. the Large Area Survey (LAS), Galactic Clusters Survey (GCS) and General Plane Survey (GPS)]. Details of the procedure are in Collins & Hambly (2012) and summarized in Lodieu et al. (2012b) for the purpose of

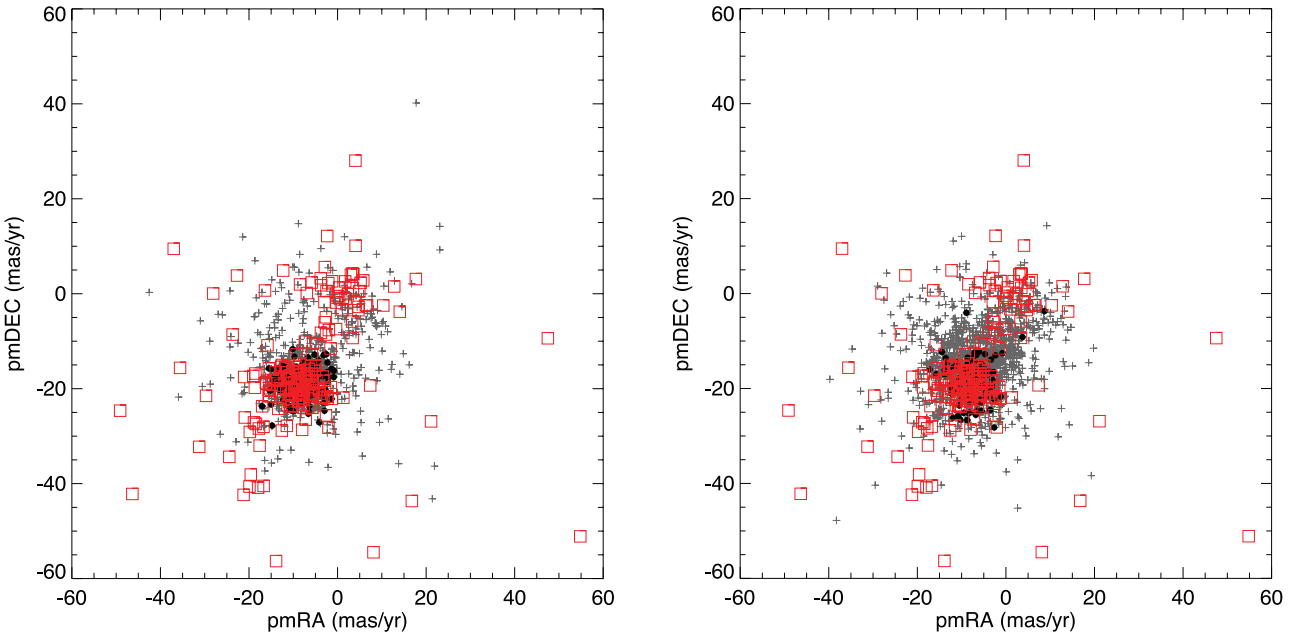

Figure 3. Vector point diagrams showing the proper motions from the GCS alone in right ascension (x-axis) and declination (y-axis) for previously known member candidates recovered by the GCS DR10 (red open squares) and all point sources after the crude photometric selection made in the ($Z - J$,Z) colour–magnitude diagram for the *ZYJHK*-PM sample. The black filled dots indicate our photometric and astrometric member candidates in USco. Left: vector point diagram for a region without extinction. Right: same diagram for the area of USco affected by reddening.

the Pleiades. The typical error bars on the GCS proper motions in USco are 4 and 6 mas yr^{-1}, down to $Z = 19$ and 20 mag, respectively (Fig. 3).

First, we applied a crude photometric selection to work with a subsample of the entire catalogue. We selected all sources located to the right of the line running from (0.5,12) to (2.2,21.5) in the ($Z - J$, Z) colour–magnitude diagram (Fig. 4). We made sure that this line allowed us to recover known spectroscopic members (see Section 3). This sample contains 29 382 sources, divided into 9351 in the region free of extinction and 20 031 in the parts affected by reddening (Fig. 1; Table 1).

The rest of the USco association is not covered with enough epochs to measure proper motions based only on GCS data. This is the case for the GCS SV (Table 1) and the area covered in *HK* only. In the case of the GCS SV area, we have *ZYJHK* photometry and proper motions measured from the 2MASS/GCS cross-match. Lodieu et al. (2007) identified member candidates in this part of the association (although with a slightly smaller area released at that time) and confirmed a large number as spectroscopic members (Lodieu et al. 2011b). Dawson et al. (2013) also included this region in their study of the disc properties of USco low-mass and brown dwarfs, as did Riaz et al. (2012). We have 430 sources in the GCS SV region, after applying the crude photometric selection described above.

We added to those samples the full coverage of the GCS DR10, only imaged in the H and K passbands (hereafter the *HK* sample). We also measured proper motions from the 2MASS/GCS correlation. Our query returned a total of 7328 848 to which we should remove the GCS SV and GCS DR10 samples as well as the region most affected by reddening (defined by RA = 245°–249.°5 and Dec. between −25.°6 and −19°, see Table 1). We applied a crude photometric selection in the ($H - K$, H) colour–magnitude diagram, keeping only sources to the right of a line running from ($H - K$, H) = (0.2,12) to (0.7,18). We are left with 39 450 sources to investigate astrometrically (Section 4.1).

3 CROSS-MATCH WITH PREVIOUS SURVEYS

We compiled a list of USco members published over the past decades by various groups (Preibisch et al. 1998, 2001; Ardila et al. 2000; Preibisch & Zinnecker 2002; Martín et al. 2004; Lodieu et al. 2006, 2007, 2008, 2011b; Slesnick et al. 2006; Dawson et al. 2011, 2013; Luhman & Mamajek 2012) to update their membership status with the photometry and astrometry provided by the GCS DR10 (Table 2). This list will serve as a starting point to identify new member candidates in the GCS, estimate the mean (relative) proper motion of USco members and derive the cluster luminosity and mass functions. We compiled a list of 2079 candidates, reduced to 1566 after removing multiple pairs.

We cross-correlated this list of 1566 known member candidates with the *ZYJHK*-PM catalogue using a matching radius of 3 arcsec and found 125 sources in common (red open squares in Fig. 3; Table 2). We repeated the same process with the GCS SV and *HK*-only areas, yielding 73 and 651 member candidates in common, respectively (Table 2). The number of known member candidates recovered in GCS DR10 is generally low because most surveys focused on the northern area with right ascensions between 240° and 245° and declinations above −25° (see the list of sources in Luhman & Mamajek 2012). Below we provide a few comments on the recovery rate for the early studies listed in Table 2.

(i) The samples published by Preibisch et al. (2001) and Preibisch & Zinnecker (2002) lie outside the GCS DR10 and SV areas and a very few objects of the X-ray and proper motion catalogues of Preibisch et al. (1998) lie in those regions as well as X-ray and proper motion samples of Preibisch et al. (1998). Most of the members from Preibisch et al. (1998, 2001) are too bright for the UKIDSS GCS and generally saturated because they are brighter than $B = 15.3$ mag and have spectral types earlier than M.

(ii) All candidates identified in the successive GCS releases by Lodieu et al. (2006, 2007) and Dawson et al. (2011, 2013) are recovered by our analysis but the assessment of their membership

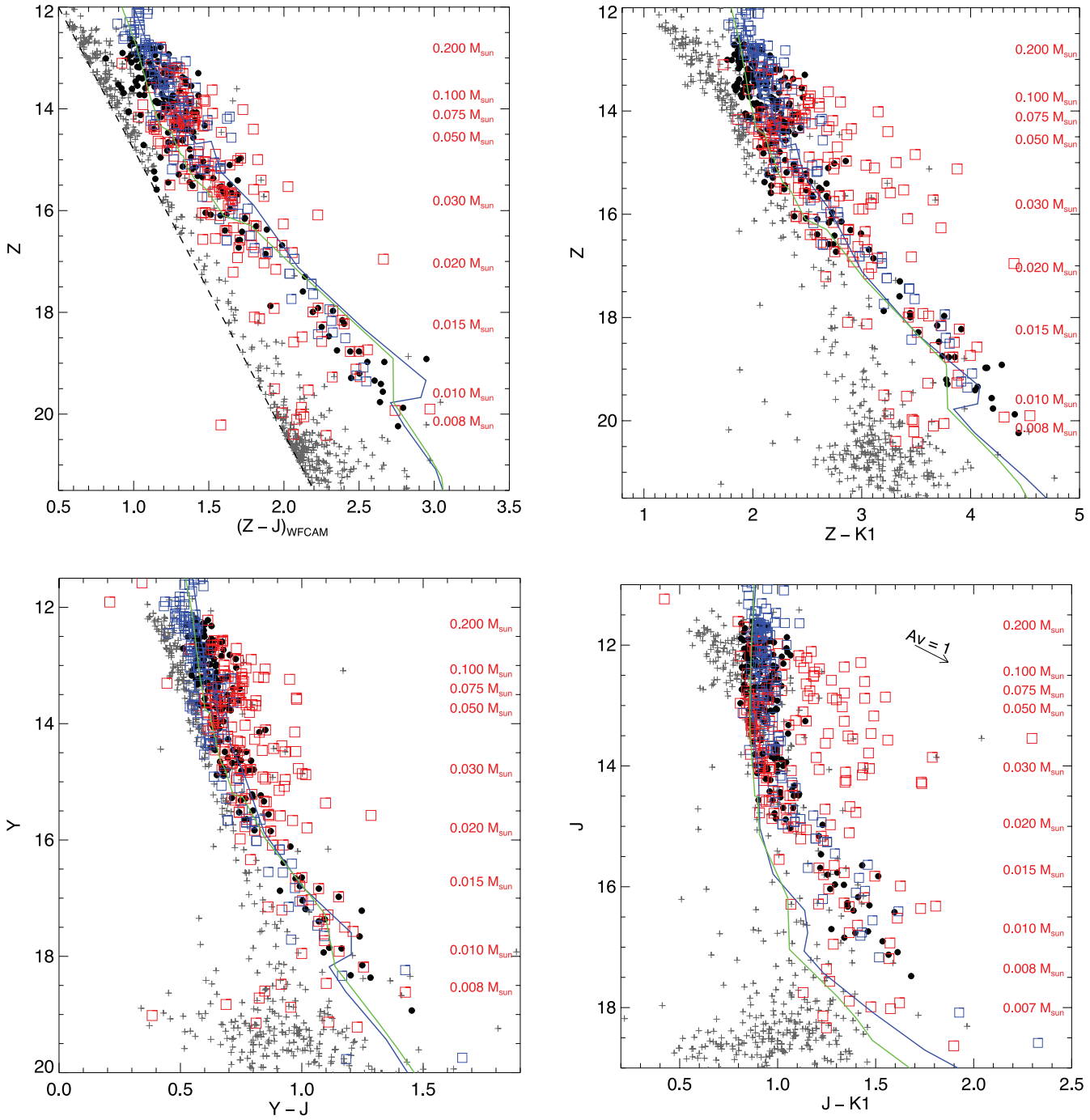

Figure 4. Colour–magnitude diagrams showing the USco member candidates previously reported in the literature (red open squares) and the new ones identified in this work (black dots). Photometric and/or proper motion non-members are highlighted as grey crosses. Known spectroscopic members are overplotted as blue open squares (Lodieu et al. 2011b). Overplotted are the 5 and 10 Myr old BT-Settl isochrones (Allard et al. 2012) shifted at a distance of 145 pc. The mass scale shown on the right-hand side of the diagrams spans approximately 0.2–0.008 $M_{\odot}$, according to the 5 Myr isochrones. The dashed line in the upper-left diagram represents our crude photometric selection using a line running from $(Z - J, Z) = (0.5,12.0)$ to $(2.2,21.5)$. Upper left: $(Z - J, Z)$; Upper right: $(Z - K, Z)$; Lower left: $(Y - J, Y)$; Lower right: $(J - K, J)$.

changes slightly following the improvement on the proper motions from the 2MASS/GCS cross-match to the two GCS epochs. They are covered by the GCS DR10 *ZYJHK*-PM and SV samples.

(iii) The full catalogue of USco members published by Luhman & Mamajek (2012) contains a total of 863 sources, including 381 brighter than $J = 11.5$ mag, which are saturated on the GCS images. Hence, our recovery rate of 405 sources out of (863−381) = 482 in the GCS is over 80 per cent. Similarly, we recovered 472 sources among the 806 with *HK* photometry, which is over 98 per cent completeness because most of the other objects are saturated in the GCS.

(iv) The recovery of candidates published by the remaining studies is mainly biased due to the lack of overlap between those surveys (red asterisks in Fig. 1) and the *ZYJHK*-PM and GCS SV. Table 2

Table 1. Approximate coordinates of the USco regions from the *ZYJHK*-PM sample with and without extinction, the GCS SV and the *HK*-only coverage (one in 100 sources shown; Fig. 1).

Region	RA (°)	Dec. (°)	Area (deg^2)
No extinction 1	≤244.4	Any	33.3
No extinction 2	≥244.4	> −22.5	3.3
Extinction 1	244.4–248.0	≤ −27	7.7
Extinction 2	244.0–246.0	−27.0 to −24.5	3.0
Extinction 3	≥246.0	−26.0 to −23.5	5.7
SV 1	241.4–244.3	−24.0 to −22.2	5.2
SV 2	241.8–243.7	−22.2 to −21.4	1.5
HK with extinction	245.0–249.5	−25.6 to −19.0	29.7

Table 2. Numbers of USco member candidates recovered in the full GCS data base using a matching radius of 3 arcsec before running our SQL queries (GCS), in the *ZYJHK*-PM sample (DR10), in the SV area (SV) and in the *HK*-only region. Papers dedicated to USco are listed below and ordered by year. References are Preibisch et al. (1998, X-ray and proper motion samples), Preibisch et al. (2001), Preibisch & Zinnecker (2002), Ardila et al. (2000), Martín et al. (2004), Slesnick et al. (2006), Lodieu et al. (2006), Lodieu et al. (2007), Lodieu et al. (2008), Dawson et al. (2011), Lodieu et al. (2011b), Dawson et al. (2013), Luhman & Mamajek (2012). The last column lists the percentage of sources in the original paper recovered in the *ZYJHK*-PM coverage with and without extinction.

Survey reference	GCS	DR10	SV	*HK*	Per cent
Preibisch1998_Xray	20/78	0/10	0/10	10/55	25.6
Preibisch1998_PM	21/115	2/20	0/1	14/89	18.3
Preibisch2001	0/100	0/0	0/0	7/100	0.0
Preibisch2002	0/166	0/0	0/0	98/166	0.0
Ardila2000	17/20	1/2	0/0	14/20	85.0
Martin2004	10/40	2/6	2/4	36/36	25.0
Slesnick2006	7/38	2/2	2/5	33/34	18.4
Lodieu2006	15/15	15/15	0/0	15/15	100.0
Lodieu2007	129/129	0/0	64/129	97/129	100.0
Slesnick2008	38/145	10/12	16/26	127/140	26.2
Dawson2011	28/28	28/28	0/0	28/28	100.0
Dawson2013	116/116	74/74	35/42	116/116	100.0
Luhman2012	405/863	47/92	65/173	472/806	46.9
Total	186/1566	125/158	73/202	651/1066	11.9

demonstrates that most of the sources published by previous studies are part of the region covered in *H*, *K*. The most incomplete recoveries are due to the bright early-type members in the catalogues of Preibisch et al. (1998, 2001) and Luhman & Mamajek (2012) as discussed in the previous points.

4 NEW USCO LOW-MASS AND BROWN DWARF MEMBER CANDIDATES

4.1 Astrometric selection

After the original photometric selection and the recovery of known member candidates, we plotted them as red open squares in Fig. 3. We observe two groups of objects, one centred on (0,0) made of field objects, and another one depicting the position of USco. We measured mean (relative) proper motions of −8.6 and −19.6 mas yr^{-1} in right ascension and declination, respectively, compared to the absolute values of −11 and −25 mas yr^{-1} from *Hipparcos* (de Bruijne et al. 1997; de Zeeuw et al. 1999). We noticed the same effect in the Pleiades (Lodieu et al. 2012b), α Per (Lodieu et al. 2012a) and Praesepe (Boudreault et al. 2012) because the GCS provides *relative* motions rather than *absolute* motions as in the case of *Hipparcos*. We applied a 3σ astrometric selection using the error bars for each source from the GCS in both directions, leaving 87 of the 186 known member candidates in the *ZYJHK*-PM sample.

We applied the same 3σ astrometric selection to the full sample of point sources towards USco, both for the sample free of extinction and the one affected by reddening. In the former case, we are left with 700 of the original 9351 sources, and, in the latter, 1357 of the 20 031 objects (grey crosses in Fig. 3). We plot these proper motion member candidates as grey crosses in the colour–magnitude diagrams displayed in Fig. 4. We tested the influence of our choice of the relative proper motion values in right ascension and declination by adding and removing 1 mas yr^{-1} in both directions (about 20 per cent of the mean error bars on the proper motions). We found that the numbers of candidates would change by less than 5.4 per cent (677 and 738 candidates in the worst cases compared to 700) and 8.3 per cent (1253 and 1468 compared to 1357) in the case of the *ZYJHK*-PM samples without and with reddening, respectively.

For the remaining areas of the association, we measured the proper motions from the 2MASS/GCS cross-match, whose accuracy is about twice worse than the GCS proper motions (10 mas yr^{-1} down to $J = 15.5$ mag). The mean proper motion of known spectroscopic members in the SV area is −8.5 and −19.2 mas yr^{-1} in right ascension and declination, respectively. As described above, those values differ from the absolute mean proper motion of USco but we used them for our 2MASS/GCS astrometric selection. We note that these values are very similar to the mean proper motions derived from the two GCS epochs. We are left with 242 sources out of the 430 original photometric candidates in the GCS SV area, after applying a 2σ selection (Table C1). Changing the mean values of the proper motions in each direction by ± 1 mas yr^{-1} results in a number of member candidates that differs by less than 3.75 per cent.

For the *HK*-only area, the situation is worse than for the SV region because we have only two bands available ($H + K$) where the cluster sequence is not so well separated from the field stars along the line of the association as in the ($Z - J$, Z) colour–magnitude diagram. Hence, our final *HK* sample will be significantly more contaminated than the aforementioned samples. First, we applied a conservative photometric selection in the ($H - K$, H) diagram by considering only point sources to the right of a line running from ($H - K$, H) = (0.2,12) to (0.7,18). After this first step, we are left with 63 520 candidates. Secondly, we applied a 2σ astrometric selection (i.e. 2 × 10 mas yr^{-1} or 95.4 per cent completeness) in the $H = 12.5$–15 mag interval (corresponding to masses ranging from 0.12–0.175 to 0.015–0.02 M$_\odot$ for ages of 5 and 10 Myr, respectively), yielding 976 candidates. Thirdly, we applied a stricter photometric selection in the ($H - K$, H) diagram, keeping sources to the right of a line running from (0.31,12.5) to (0.7,16.5). This line was chosen to recover all photometric and astrometric candidates from the SV-only and *ZYJHK*-PM samples. We are left with 286 candidates in the *HK* region (Fig. 1; Table D1). We tested the influence of our astrometric selection by changing the mean proper motion in RA and Dec. by ± 1 mas yr^{-1}, yielding in the extreme cases 281 and 304 candidates, i.e. a difference of 6.3 per cent in the worst case compared to our original choice. The main uncertainty on the number of candidates in the *HK*-only sample rather comes from the choice of the sigma in the astrometric selection: choosing 2.5σ (99 per cent completeness) and 3σ (99.9 per cent completeness) would lead to 360 and 412 candidates, respectively.

4.2 Photometric selection

To further refine our list of USco member candidates, we applied additional photometric cuts in various colour–magnitude diagrams for the *ZYJHK*-PM sample, defined as follows:

(i) $(Z-K, Z) = (1.60,12.0)$ to $(2.20,16.0)$
(ii) $(Z-K, Z) = (2.20,16.0)$ to $(4.00,20.0)$
(iii) $(Y-J, Y) = (0.40,12.0)$ to $(0.65,15.0)$
(iv) $(Y-J, Y) = (0.65,15.0)$ to $(1.00,18.0)$
(v) $(J-K, J) = (0.80,11.5)$ to $(0.80,14.0)$
(vi) $(J-K, J) = (0.80,14.0)$ to $(1.40,18.0)$.

The numbers of candidates after the $Z-K$, $Y-J$ and $J-K$ photometric selections are 279, 257 and 252, respectively, demonstrating that the most influential criteria are the astrometric and $Z-K$ selections. Indeed, the additional $Y-J$ and $J-K$ selection remove small numbers of cluster member candidates. We stress that these cuts were chosen to recover known spectroscopic members from earlier surveys (see Section 3). These photometric selections returned 252 candidates in the region free of extinction (filled black dots in Fig. 4) and 396 in the region affected by reddening (filled black dots in Fig. 5). Similarly, we identified 84 member candidates in the SV region of the GCS.

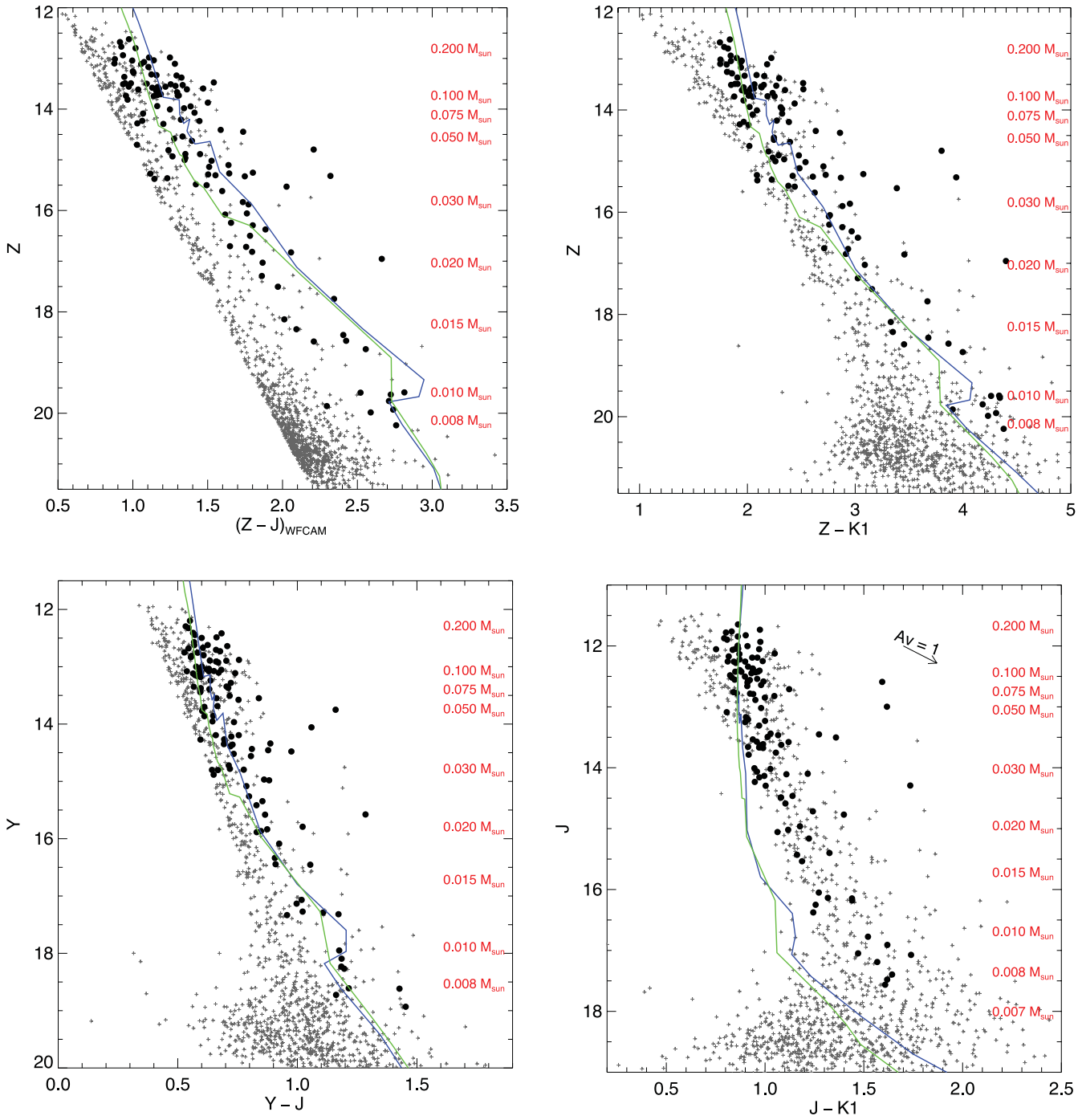

Figure 5. Same as Fig. 4 but for the region in USco affected by reddening.

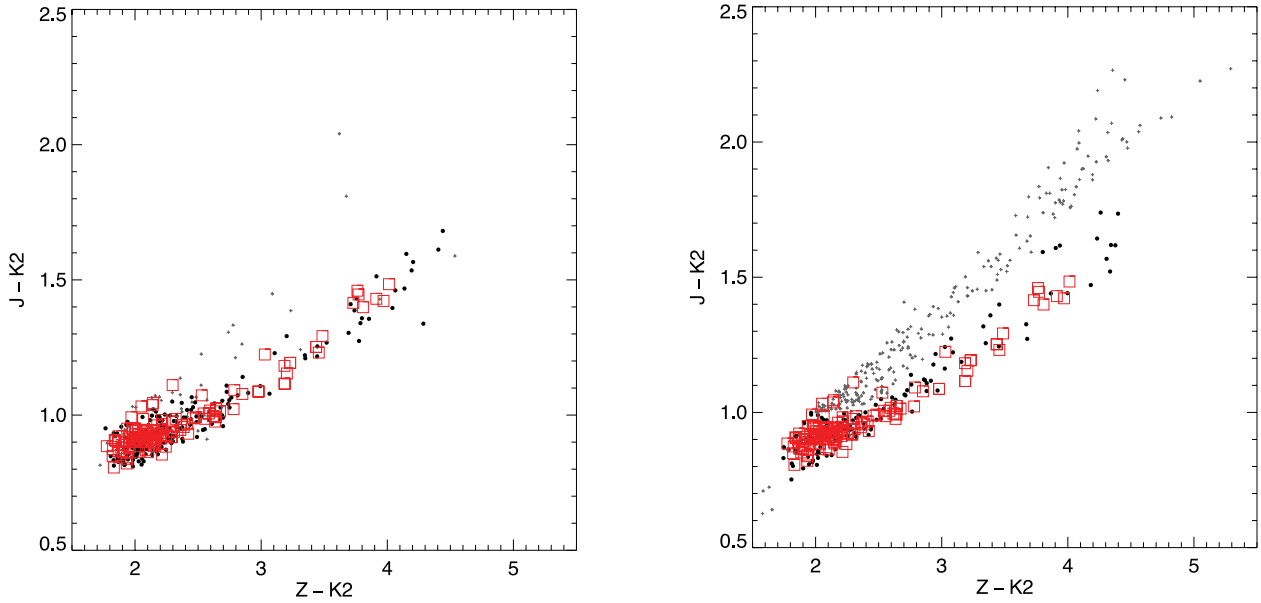

Figure 6. $(Z-K, J-K)$ colour–colour diagram for the photometric and astrometric candidates (grey crosses) in the region free of extinction (left) and the region affected by reddening (right) of the *ZYJHK*-PM sample. Overplotted as red open squares are known spectroscopic members. USco candidate members identified in our study are plotted as black dots.

We tested the influence of the choice of our selection lines on the final numbers of candidates, in the specific case of the *ZYJHK*-PM sample without extinction. We shifted each selection line to the left and to the right by 0.1 mag, which corresponds roughly to the error on the colour (i.e. 1σ) at the faint end of the sequence at $J = 18$ mag. This shift corresponds to 2.5σ at $J = 17$ mag. We found that the shift to the blue of the six selection lines enumerated above yields roughly 20–30 per cent more cluster member candidates. Similarly, a shift to the red gives about 20 per cent less candidates in the $(Z-K, Z)$ diagram and 41–43 per cent less in the other two diagrams.

We know that the level of contamination will be high in the region affected by reddening. Hence, we applied an additional photometric criterion in the $(Z-K, J-K)$ two-colour diagram (Fig. 6) to remove giants and reddened stars based on the location of previously known spectroscopic members (red open squares; Lodieu et al. 2011b). We selected sources satisfying the following criteria:

(i) $(J-K) \geq 1.0$ for $(Z-K)$ between 1.7 and 2.4,
(ii) sources below the line defined by $(Z-K, J-K) = (2.4,1.0)$ and (4.4,1.85).

This selection returned 201 and 120 sources (corresponding to 80 and 30 per cent of the candidates left after the astrometric and the first three photometric selections) in the region with and without reddening, respectively. Only two candidates (or 2.5 per cent) were rejected in the SV sample after applying this additional criterion. We list the coordinates, photometry and proper motions of the candidates identified in *ZYJHK*-PM (including known members published by other groups) in Tables A1 and B1 for the regions with and without reddening, respectively. We display their distribution in Fig. 1. We provide the list of member candidates within the SV area in Table C1.

We tested the influence of the choice of the crude selection in the $(Z-J, Z)$ colour–magnitude diagram by choosing a line shifted by 0.1 mag to the left of the original choice. We applied again the same aforementioned criteria and arrived at the same numbers of candidates for the two *ZYJHK*-PM samples and the SV-only sample.

4.3 Catalogue summary

To summarize, we have identified a total of 688 sources in four different regions within USco: 195 and 111 in the *ZYJHK*-PM regions without reddening and with extinction, 79 in the SV area and 276 in the *HK*-only region. We found 11 sources in common among them, leaving 677 USco member candidates. We cross-matched this list with itself and found 4, 12 and 15 sources within 10, 50 and 100 arcsec of each other, pointing towards binary fractions for wide common proper motions of 0.6, 1.8 and 2.2 per cent for projected separations of 1450, 7250 and 14500 au, respectively.

5 VARIABILITY AT YOUNG AGES

We investigate the variability of low-mass stars and brown dwarfs in USco using the two *K*-band epochs provided by the GCS. Fig. 7 shows the $(K1–K2)$ versus $K2$ diagram for USco member candidates in the *ZYJHK*-PM sample. This analysis is not possible for the SV sample because no second *K*-band epoch is available.

The brightening in the $K1 = 10.5–11.5$ mag range is due to the difference in saturation between the first and second epochs, of the order of 0.5 mag both in the saturation and completeness limit. This is understandable because the exposure times have been doubled for the second epoch with relaxed constraints on the seeing requirement and weather conditions. We excluded those objects from our variability study. Overall, the sequence indicates consistent photometry between the two *K* epochs with a very few objects being variable.

At first glance, we spotted four potential variables in Fig. 7 (Table 3). The GCS images do not show anything anomalous so we did not proceed further. We selected variable objects by looking at the standard deviation, defined as 1.48 times the median absolute deviation which is the median of the sorted set of absolute values of deviation from the central value of the $K1 - K2$ colour. We identified one potential variable object with a difference of 0.37 mag in the 11.5–12 mag range, whereas the other three fainter candidates with differences between 0.1 and 0.16 mag lie just below the 3σ

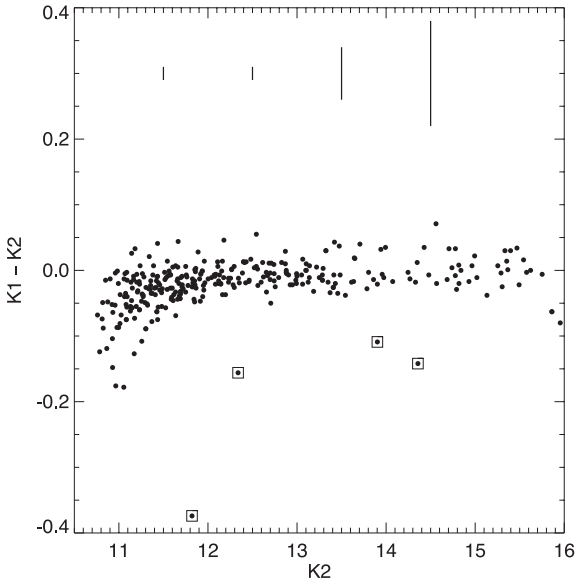

Figure 7. Difference in the K magnitude ($K1$–$K2$) as a function of the $K2$ magnitude for all USco member candidates with proper motions from GCS DR10. The four potential variable sources are highlighted with large open squares. Typical error bars on the colour shown as vertical dotted lines are added at the top of the plot.

Table 3. Potential variable candidates in our USco *ZYJHK*-PM sample of low-mass stars and brown dwarfs.

RA	Dec.	$K1$	$K2$	ΔK
15:52:33.93	−26:51:12.4	11.447	11.821	−0.374
16:23:23.06	−29:01:33.4	12.182	12.338	−0.156
15:47:22.82	−21:39:14.3	14.215	14.357	−0.142
16:23:22.02	−26:09:55.6	13.793	13.902	−0.109

of the median absolute deviations of 0.05–0.06 mag. These small variations of the order of 0.1–0.15 mag can be interpreted by the presence of cool spots in low-mass stars (e.g. Scholz et al. 2009).

We conclude that the level of K-band variability at 5–10 Myr is small, with standard deviations of the order of 0.06 mag range, suggesting that it cannot account for the dispersion in the cluster sequence. We arrived at the same conclusions in the case of the Pleiades (Lodieu et al. 2012b), α Per (Lodieu et al. 2012a) and Praesepe (Boudreault et al. 2012) although these clusters are older (85, 120 and 590 Myr, respectively).

6 DISC FREQUENCY IN USCO

We cross-correlated our lists of candidates with the *Wide-field Infrared Survey Explorer* (*WISE*) all-sky release (Wright et al. 2010) using a matching radius of 3 arcsec. We found a total of 660 matches, divided into 194 in the *ZYJHK*-PM, 111 in the *ZYJHK*-PM region with extinction, 79 objects in the SV-only area and 276 counterparts in the *HK*-only region, respectively (Table E1). We looked at the *WISE* images and found that all *WISE* counterparts to the GCS objects are detected in $w1$ and $w2$. We classified the sources listed in Table E1 in two categories: 224 (33.9 per cent) source detections in $w3$ but not in $w4$ and 58 (8.8 per cent) objects detected in $w3$ and $w4$ marked as 1110 (open triangles in Fig. 8) and 1111 (open squares in Fig. 8), respectively. The latter objects detected in all *WISE* bands are unambiguous disc-bearing low-mass stars and brown dwarfs.

We considered two different methods to estimate the disc frequency of USco members with masses below 0.2 $M_{\odot}$, according to the BT-Settl models (Allard et al. 2012). We plot in Fig. 8 the ($w1 - w2$, K) and ($K - w1$, $w1 - w3$) diagrams. The former represents a good discriminant to separate disc-less and disc-bearing objects according to Dawson et al. (2013). We note that we chose K as the infrared band rather than J as in Dawson et al. (2013) because all targets in our four samples have K-band photometry. This diagram is efficient in Taurus but may not be the best criterion for USco where many transition discs are found (Riaz et al. 2012). The ($K - w1$, $w1 - w3$) colour–colour diagram, however, clearly separates

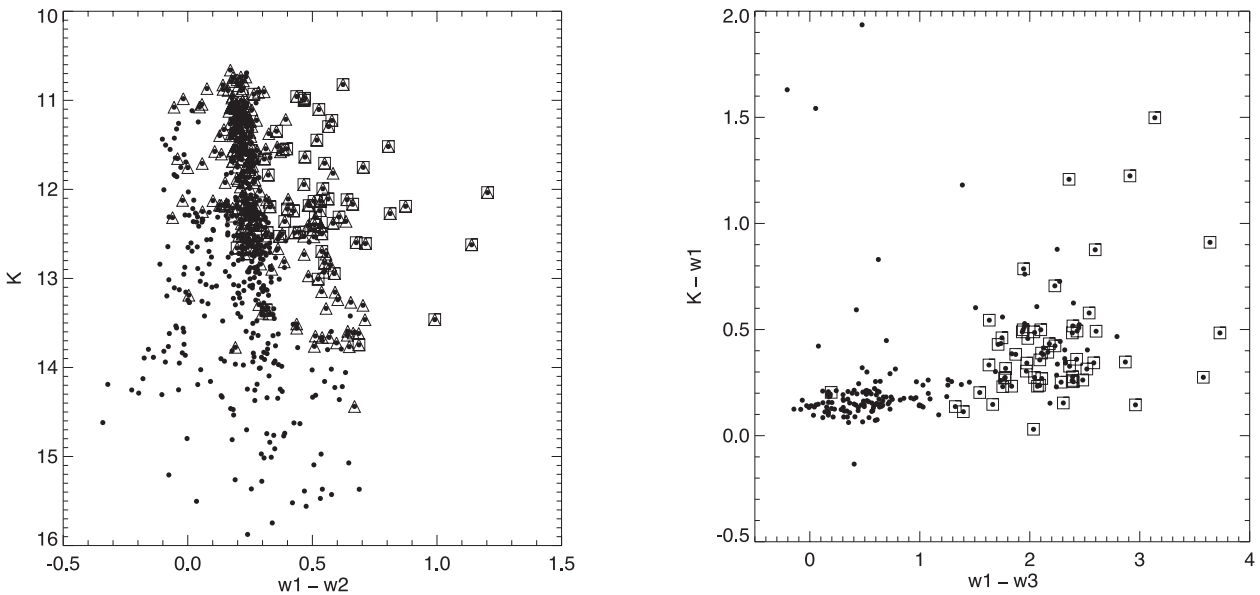

Figure 8. ($w1 - w2$, K) and ($w1 - w3$, $K - w1$) diagrams for USco members with *WISE* counterparts (black dots). The open triangles and open squares denote sources detected in $w3$ and $w3 + w4$, respectively.

brown dwarf and M dwarf discs (Peña Ramírez et al. 2012) as well as primordial discs in USco (fig. 5 of Riaz et al. 2012).

We observe three sequences in the ($w1 - w2$, K) diagram (left-hand panel of Fig. 8): one sequence to the left likely made of non-members mainly from the *ZYJHK*-PM region with extinction and the *HK*-only area where our contamination is expected to be higher than in the other two areas (*ZYJHK*-PM without reddening and SV-only). Optical spectroscopy is needed to confirm our claims though. Broadly, we have the same number of sources with discs (16 per cent or 107 sources with $w1 - w2 \geq 0.4$ mag) as potential contaminants (100 sources or 15 per cent with $w1 - w2 \leq 0.1$ mag), implying that the frequency of disc-bearing USco members lies between 107/600 = 16.2 per cent and 107/(660−100) = 19.1 per cent, following the arguments of Dawson et al. (2013). However, these numbers are lower limits because 17/58 (29.3 per cent) $w3 + w4$ detections have $w1 + w2$ colours bluer than 0.4 mag, i.e. lie in the middle sequence, yielding corrected disc fractions of 18.8 and 22.1 per cent. We are certainly missing some disc-bearing members hiding among $w3$ detections but they are difficult to quantify without a cautious fitting of the spectral energy distributions (beyond the scope of this paper), as discussed in details in Riaz, Lodieu & Gizis (2009) and Dawson et al. (2013). Nonetheless, we can place an upper limit of (224+58)/660 = 42.7 per cent on the overall disc fraction for USco low-mass stars and brown dwarfs. Similarly, we can set a lower limit of 6/58 = 10 per cent based on the six unambiguous disc objects with $w1 + w2 \geq 0.8$ among sources detected in all four *WISE* bands.

We observe two groups of objects in the ($K - w1$, $w1 - w3$) diagram (right-hand panel of Fig. 8) depicting photospheric sources ($w1 - w3 \leq 1.2$ mag) and disc-bearing members ($w1 - w3 \geq 1.5$ mag). Objects in the middle may be good candidates to transition discs (Riaz et al. 2012). Among the 282 USco member candidates detected in three or four *WISE* bands, we have 89 sources with $w1 - w3 \geq 1.5$ mag, implying a disc fraction of 31.5 per cent (most likely range of 26.6–37.1 per cent). This fraction would increase by 5 per cent if we include the potential transition discs.

The disc frequencies derived by both methods are consistent within the error bars although the second one is on average higher. Our values should be compared with the 23 ± 5 per cent of Dawson et al. (2013) for USco brown dwarfs and 25 ± 3 per cent of Luhman & Mamajek (2012) for M4–L2 members. For earlier type members the disc, fractions range from 10 per cent for K0–M0 dwarfs (Luhman & Mamajek 2012) to 19 per cent for K0–M5 dwarfs (Carpenter et al. 2006). Our disc fraction for USco substellar members is consistent with the 42 ± 12 and 36 ± 8 per cent disc frequencies for brown dwarfs in IC 348 (1–3 Myr; Luhman et al. 2005) and σ Orionis (1–8 Myr; Peña Ramírez et al. 2012).

7 THE INITIAL MASS FUNCTION

We derive the cluster luminosity and system mass functions from our astrometric and photometric sample of ∼320 USco member candidates distributed over ∼50 square degrees (the *ZYJHK*-PM sample). We did not attempt to correct the mass function for binaries for two reasons. First, the presence of discs around USco low-mass stars and brown dwarfs tends to displace these sources to the right-hand side of the sequence, implying that disentangling binaries from disc-bearing members is difficult than in the case of more mature clusters like the Pleiades (Lodieu et al. 2012b) and Praesepe (Boudreault et al. 2012). Secondly, a recent high-resolution imaging survey of 20 USco spectroscopic members fainter than $J = 15$ mag by Biller et al. (2011) resolved only one binary, pointing towards a binary frequency lower than 10 per cent. This fraction is lower than the uncertainty on the number of sources per mass bin at the low-mass end, assuming Gehrels error bars.

7.1 The age of USco

de Zeeuw & Brand (1985) and de Geus, de Zeeuw & Lub (1989) derived an age of 5–6 Myr comparing sets of photometric data with theoretical isochrones available at that time. Later, Preibisch & Zinnecker (1999) confirmed that USco is likely 5 Myr old with a small dispersion on the age by placing about 100 spectroscopic members on the Hertzsprung–Russell diagram. This age estimate was later supported by Slesnick et al. (2008) from a wide-field optical study of low-mass stars and brown dwarfs with spectroscopic membership: these authors derived a mean age of 5 Myr with an uncertainty of 3 Myr taking into account all possible sources of uncertainties. More recently, Pecaut et al. (2012) argued for an age older (11 ± 2 Myr) from an analysis of the F-type members of the full Scorpius–Centaurus association. They determined older ages for all three subgroups forming Scorpius–Centaurus, including ages of 16 and 17 Myr for Upper Centaurus–Lupus and Lower Centaurus–Crux, which are older than the ages derived by Song et al. (2012) from the abundances of lithium in the spectra of F/K members of the association.

In this work, we adopt an age of 5 Myr for USco but we will also investigate the influence of age on the shape of the mass function (Section 7.3).

7.2 The cluster luminosity function

We construct the cluster luminosity function from our astrometric and photometric *ZYJHK*-PM sample of 320 candidate members spanning $J = 11$–17.5 mag. We display the luminosity function divided into bins of 0.5 mag in the left-hand panel of Fig. 9 with Gehrels error bars (Gehrels 1986). We note that the first and last bins are lower limits because of incompleteness at the bright and faint ends. We observe that the number of objects decreases with fainter magnitudes, i.e. cooler temperatures.

7.3 The cluster mass function

We adopt the logarithmic form of the initial mass function as originally proposed by Salpeter (1955): $\xi(\log_{10}m) = \mathrm{d}n/\mathrm{d}\log_{10}(m) \propto m^{-\alpha}$. We converted the luminosity into a mass using the BT-Settl models (Allard et al. 2012) and the J-band filter for all sources. We assumed a distance of 145 pc (van Leeuwen 2009) and an age of 5 Myr for USco (Table 4). We also considered an age of 10 Myr to compute the mass function (Table 5), keeping the same magnitude bins as a starting point.

We compare in Fig. 9 the mass function derived from our *ZYJHK*-PM sample with the previous sample of spectroscopic members presented in Lodieu et al. (2011b). We emphasize that the first and last bins are incomplete because of saturation on the bright side and incompleteness on the faint side. Both mass functions were computed assuming an age of 5 Myr but the earlier determination made use of the NextGen (Baraffe et al. 1998) and DUSTY (Chabrier et al. 2000) whereas we use the BT-Settl (Allard et al. 2012) with the new data set presented here. Nonetheless, we observe that both mass functions are similar, with a possible excess of brown dwarfs below ∼0.03 $M_{\odot}$ as originally claimed by Preibisch et al. (2001) and Slesnick et al. (2008). This excess of substellar objects is enhanced

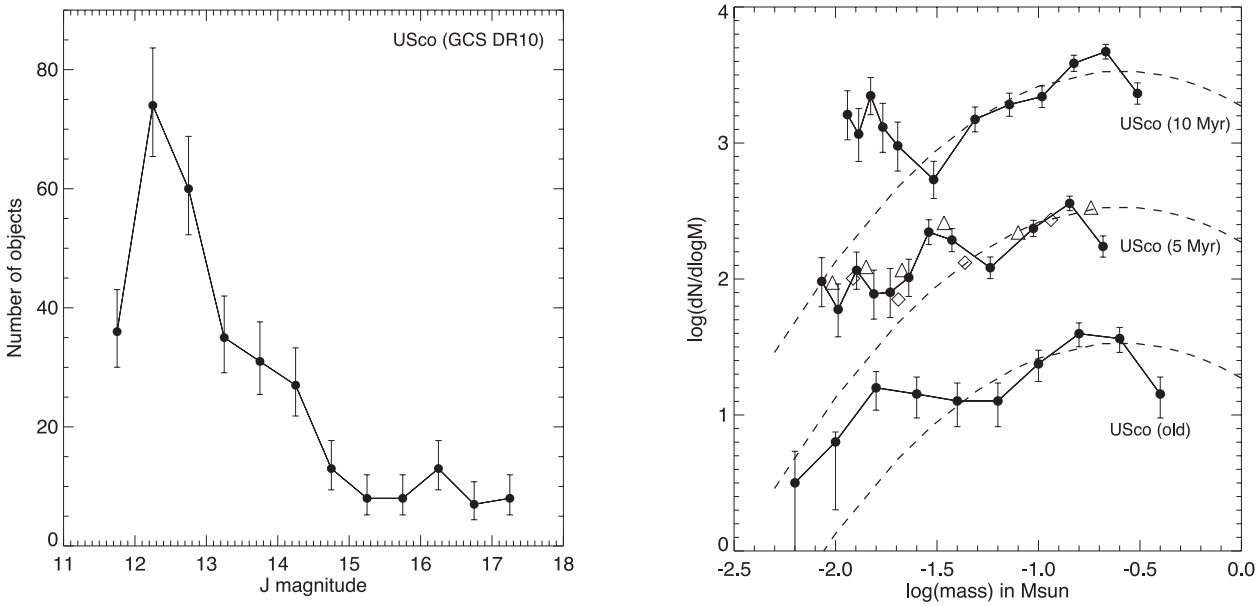

Figure 9. Luminosity (left) and mass (right) functions derived from our *ZYJHK*-PM sample of USco member candidates. We plot the mass function for 5 and 10 Myr, ages quoted in the literature for USco as well as the mass function derived from the spectroscopic sample of Lodieu et al. (2011b). Overplotted as a dashed line is the log-normal field mass function (Chabrier 2005). The binned mass functions are shown as open triangles (six bins) and open diamonds (four bins).

Table 4. Values for the luminosity and mass functions for USco for an age of 5 Myr. We assumed a distance of 145 pc and employed the BT-Settl theoretical isochrones to transform magnitudes into masses (Allard et al. 2012). The mass function is plotted in Fig. 9.

Mag range	Nb_obj	Mass range	Mid-mass	d*N*	err*H*	err*L*	dlog*M*	err*H*	err*L*	d*N*/d*M*	err*H*	err*L*
11.5–12.0	36	0.2470–0.1690	0.2080	36.00	7.06	5.98	461.54	90.54	76.66	2.34	0.18	0.18
12.0–12.5	74	0.1690–0.1160	0.1425	74.00	9.65	8.59	1396.23	182.00	162.03	2.66	0.12	0.12
12.5–13.0	60	0.1160–0.0728	0.0944	60.00	8.79	7.73	1388.89	203.57	178.93	2.47	0.14	0.14
13.0–13.5	35	0.0728–0.0429	0.0578	35.00	6.98	5.89	1170.57	233.42	197.15	2.18	0.18	0.18
13.5–14.0	31	0.0429–0.0320	0.0374	31.00	6.63	5.55	2844.04	608.69	508.74	2.39	0.19	0.20
14.0–14.5	27	0.0320–0.0256	0.0288	27.00	6.27	5.17	4218.75	979.35	808.13	2.45	0.21	0.21
14.5–15.0	13	0.0256–0.0203	0.0230	13.00	4.71	3.57	2452.83	888.32	673.72	2.11	0.31	0.32
15.0–15.5	8	0.0203–0.0169	0.0186	8.00	3.96	2.78	2352.94	1164.13	818.79	2.00	0.40	0.43
15.5–16.0	8	0.0169–0.0140	0.0155	8.00	3.96	2.78	2758.62	1364.84	959.96	1.99	0.40	0.43
16.0–16.5	13	0.0140–0.0114	0.0127	13.00	4.71	3.57	5000.00	1810.81	1373.35	2.16	0.31	0.32
16.5–17.0	7	0.0114–0.0092	0.0103	7.00	3.78	2.60	3181.82	1719.95	1180.94	1.88	0.43	0.46
17.0–17.5	8	0.0092–0.0079	0.0086	8.00	3.96	2.78	6153.85	3044.65	2141.45	2.08	0.40	0.43

Table 5. Values for the luminosity and mass functions for USco for an age of 10 Myr. We assumed a distance of 145 pc and employed the BT-Settl theoretical isochrones to transform magnitudes into masses (Allard et al. 2012). The mass function is plotted in Fig. 9.

Mag range	Nb_obj	Mass range	Mid-mass	d*N*	err*H*	err*L*	dlog*M*	err*H*	err*L*	d*N*/d*M*	err*H*	err*L*
11.5–12.0	36	0.3620–0.2530	0.3075	36.00	7.06	5.98	330.28	64.79	54.85	2.36	0.18	0.18
12.0–12.5	74	0.2530–0.1760	0.2145	74.00	9.65	8.59	961.04	125.27	111.53	2.67	0.12	0.12
12.5–13.0	60	0.1760–0.1230	0.1495	60.00	8.79	7.73	1132.08	165.93	145.85	2.59	0.14	0.14
13.0–13.5	35	0.1230–0.0852	0.1041	35.00	6.98	5.89	925.93	184.63	155.95	2.34	0.18	0.18
13.5–14.0	31	0.0852–0.0587	0.0720	31.00	6.63	5.55	1169.81	250.37	209.26	2.28	0.19	0.20
14.0–14.5	27	0.0587–0.0387	0.0487	27.00	6.27	5.17	1350.00	313.39	258.60	2.17	0.21	0.21
14.5–15.0	13	0.0387–0.0222	0.0305	13.00	4.71	3.57	787.88	285.34	216.41	1.73	0.31	0.32
15.0–15.5	8	0.0222–0.0183	0.0203	8.00	3.96	2.78	2051.28	1014.88	713.82	1.98	0.40	0.43
15.5–16.0	8	0.0183–0.0159	0.0171	8.00	3.96	2.78	3333.33	1649.18	1159.95	2.12	0.40	0.43
16.0–16.5	13	0.0159–0.0139	0.0149	13.00	4.71	3.57	6500.00	2354.05	1785.36	2.35	0.31	0.32
16.5–17.0	7	0.0139–0.0121	0.0130	7.00	3.78	2.60	3888.89	2102.16	1443.38	2.07	0.43	0.46
17.0–17.5	8	0.0121–0.0108	0.0115	8.00	3.96	2.78	6153.85	3044.65	2141.45	2.21	0.40	0.43

if we consider an age of 10 Myr although it may be the result of the mass–luminosity relation, which does not reproduce the M7/M8 gap proposed by Dobbie et al. (2002) occurring around 0.015–0.02 $M_\odot$ in USco (left-hand panel in Fig. 9). Masses of brown dwarfs at 10 Myr are higher than at 5 Myr, making the number of substellar objects piling up at higher masses, causing an enhanced bump in the mass function. We computed the mass function using ages of 3 and 1 Myr and found that the excess of brown dwarfs seems to disappear only if the association is for 1 Myr, which is lower than any age estimate from previous studies. We observe that the high-mass part (>0.03 $M_\odot$) of the USco mass function is well reproduced by the log-normal form of the field mass function (Chabrier 2003, 2005), independently of the age chosen for USco (see Section 7.1).

We investigated the role of the bin size on the shape of the mass function, assuming an age of 5 Myr and a distance of 145 pc. We considered two options: on one hand, we binned the mass function by a factor of 2, i.e. 6 bins instead of 12 (open triangles in Fig. 9), and, on the other hand, we employed 4 bins (open diamonds in Fig. 9) after removing the first and last bins which are incomplete (Table 4). We conclude that, overall, the bin size does not affect the shape of the mass function and the possible presence of the excess of low-mass brown dwarfs.

7.4 Comparison with other clusters

Fig. 10 compares the USco mass function with our studies of the Pleiades (red open triangles; Lodieu et al. 2012b) and σ Orionis (blue open squares; Lodieu et al. 2009). We note that the USco mass function is derived using the latest BT-Settl models (Allard et al. 2012), where former studies of the Pleiades and σ Orionis employed the NextGen (Baraffe et al. 1998) and DUSTY (Chabrier et al. 2000) models. The mass function of the Pleiades comes from a photometric and astrometric selection using GCS DR9 in the same manner as this work in USco. Both mass functions are very comparable in the interval where they overlap, from ∼0.2 down to ∼0.03 $M_\odot$ and match the log-normal form of the field mass function (Chabrier 2005). We note that the Pleiades mass function is comparable to the mass functions in α Per (Lodieu et al. 2012a) and Praesepe (Boudreault et al. 2012) using the same GCS DR9 data base in an homogeneous manner. This result is in line with the numerous mass functions plotted in fig. 3 of Bastian et al. (2010), demonstrating the similarities between mass functions in many clusters over a broad range of masses.

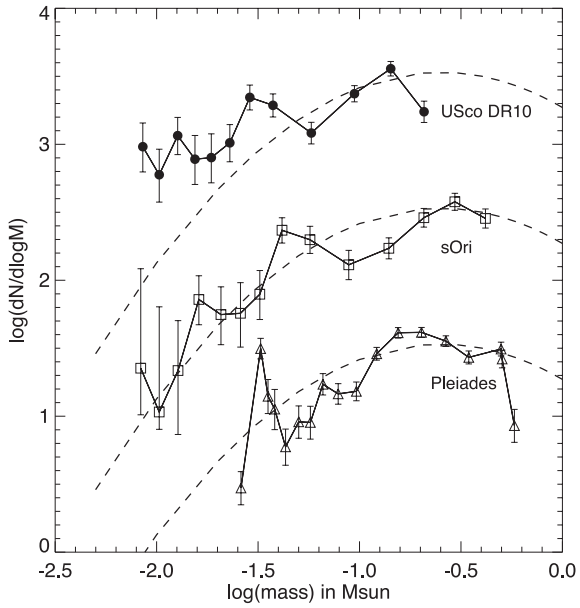

Figure 10. Mass function of USco derived from our GCS DR10 sample compared to the Pleiades (red open triangles; Lodieu et al. 2012b) and σ Orionis (blue open squares; Lodieu et al. 2009). Overplotted as a black dashed line is the log-normal field mass function (Chabrier 2005).

We plot in Fig. 10 the mass function for the young (1–8 Myr) σ Ori cluster derived from a pure photometric study using the fourth data release of the GCS (blue open squares; Lodieu et al. 2009). The shape of the σ Ori mass function agrees with the field mass function in the 0.2–0.01 $M_\odot$ mass range, as noted by independent studies of the cluster (Béjar et al. 2001, 2011; Caballero et al. 2007; Bihain et al. 2009; Peña Ramírez et al. 2012).

8 SUMMARY

We have presented the outcome of a deep and wide photometric and proper motion survey in the USco association as part of the UKIDSS GCS DR10. The main results of our analysis are as follows.

(i) We recovered several hundred known USco members and updated their membership with the proper motion and photometry available from GCS DR10.

(ii) We selected photometrically and astrometrically new potential USco member candidates and identified about 700 candidates within regions free of extinction and regions affected by reddening.

(iii) We derived the luminosity function in the USco association in the $J = 11.5$–17.5 mag range.

(iv) We derived the USco mass function which matches well the log-normal form of the system field mass function down to 0.03 $M_\odot$. The USco mass function is consistent with the Pleiades, α Per and Praesepe mass functions in the 0.2–0.03 $M_\odot$ mass range. We observe a possible excess of substellar members below 0.03 $M_\odot$, as pointed out by earlier studies (Preibisch et al. 2001; Lodieu et al. 2007; Slesnick et al. 2008), which may be due to the uncertainties on the mass–luminosity relation at the *M*/*L* transition and the age of the association.

This paper provides a full catalogue of photometric and astrometric members from 0.2 down to ∼0.01 $M_\odot$ in the southern part of the USco association. This catalogue is complemented by a complete census of the stellar and substellar populations in the full USco association down to 0.02–0.015 $M_\odot$. This work will represent a reference for many years to come. We foresee further improvement when a second epoch will be obtained for the northern part of the association as part of the Visible and Infrared Survey Telescope for Astronomy (VISTA) hemisphere survey (Emerson et al. 2004; Dalton et al. 2006). Our study provides a legacy sample that can be used to study the disc properties of low-mass stars and brown dwarfs in USco (Carpenter et al. 2006; Scholz et al. 2007; Riaz et al. 2009; Luhman & Mamajek 2012; Dawson et al. 2013), their binary properties (Biller et al. 2011) and their distribution in the association as a function of spectral type once a complete spectroscopic follow-up is available.

ACKNOWLEDGEMENTS

NL is funded by the Ramón y Cajal fellowship number 08-303-01-02 and the national programme AYA2010-19136 funded by the Spanish ministry of science and innovation. The author thanks the anonymous referee for her/his constructive and quick report. This

work is based in part on data obtained as part of the UKIRT Infrared Deep Sky Survey (UKIDSS). The UKIDSS project is defined in Lawrence et al. (2007). UKIDSS uses the UKIRT Wide Field Camera (WFCAM; Casali et al. 2007). The photometric system is described in Hewett et al. (2006), and the calibration is described in Hodgkin et al. (2009). The pipeline processing and science archive are described in Irwin et al. (2004) and Hambly et al. (2008), respectively. The author also thanks the colleagues at the UK Astronomy Technology Centre, the Joint Astronomy Centre in Hawaii, the Cambridge Astronomical Survey and Edinburgh Wide Field Astronomy Units for building and operating WFCAM and its associated data flow system. The author is grateful to France Allard for placing her latest BT-Settl models on a free webpage for the community.

This research has made use of the Simbad data base, operated at the Centre de Données Astronomiques de Strasbourg (CDS), and of NASA's Astrophysics Data System Bibliographic Services (ADS).

This publication makes use of data products from the Two Micron All Sky Survey (2MASS), which is a joint project of the University of Massachusetts and the Infrared Processing and Analysis Center/California Institute of Technology, funded by the National Aeronautics and Space Administration and the National Science Foundation.

REFERENCES

Allard F., Homeier D., Freytag B., 2012, R. Soc. Lond. Philos. Trans. Ser. A, 370, 2765
Ardila D., Martín E., Basri G., 2000, AJ, 120, 479
Baraffe I., Chabrier G., Allard F., Hauschildt P. H., 1998, A&A, 337, 403
Bastian N., Covey K. R., Meyer M. R., 2010, ARA&A, 48, 339
Béjar V. J. S. et al., 2001, ApJ, 556, 830
Béjar V. J. S., Zapatero Osorio M. R., Rebolo R., Caballero J. A., Barrado D., Martín E. L., Mundt R., Bailer-Jones C. A. L., 2011, ApJ, 743, 64
Bihain G. et al., 2009, A&A, 506, 1169
Biller B., Allers K., Liu M., Close L. M., Dupuy T., 2011, ApJ, 730, 39
Boudreault S., Lodieu N., Deacon N. R., Hambly N. C., 2012, MNRAS, 426, 3419
Caballero J. A. et al., 2007, A&A, 470, 903
Carpenter J. M., Mamajek E. E., Hillenbrand L. A., Meyer M. R., 2006, ApJ, 651, L49
Casali M. et al., 2007, A&A, 467, 777
Chabrier G., 2003, PASP, 115, 763
Chabrier G., 2005, in Corbelli E., Palla F., Zinnecker H., eds, Astrophysics and Space Science Library, Vol. 327, The Initial Mass Function 50 Years Later. Springer, Dordrecht, p. 41
Chabrier G., Baraffe I., Allard F., Hauschildt P., 2000, ApJ, 542, 464
Collins R., Hambly N., 2012, in Ballester P., Egret D., eds, ASP Conf. Ser. Vol. 461, Astronomical Data Analysis Software and Systems XXI. Astron. Soc. Pac., San Francisco, p. 525
Dalton G. B. et al., 2006, in McLean, I. S., Iye M., eds, Proc. SPIE Vol. 6269, Ground-based and Airborne Instrumentation for Astronomy. SPIE, Bellingham, p. 62690X
Dawson P., Scholz A., Ray T. P., 2011, MNRAS, 418, 1231
Dawson P., Scholz A., Ray T. P., Marsh K. A., Wood K., Natta A., Padgett D., Ressler M. E., 2013, MNRAS, 429, 963
de Bruijne J. H. J., Hoogerwerf R., Brown A. G. A., Aguilar L. A., de Zeeuw P. T., 1997, in ESA SP-402: Hipparcos - Venice '97, Improved Methods for Identifying Moving Groups. ESA, Noordwijk, p. 575
de Geus E. J., de Zeeuw P. T., Lub J., 1989, A&A, 216, 44
de Zeeuw T., Brand J., 1985, in Boland W., van Woerden H., eds, Astrophysics and Space Science Library, Vol. 120, Birth and Evolution of Massive Stars and Stellar Groups. Reidel, Dordrecht, p. 95
de Zeeuw P. T., Hoogerwerf R., de Bruijne J. H. J., Brown A. G. A., Blaauw A., 1999, AJ, 117, 354
Dobbie P. D., Pinfield D. J., Jameson R. F., Hodgkin S. T., 2002, MNRAS, 335, L79
Emerson J. P., Sutherland W. J., McPherson A. M., Craig S. C., Dalton G. B., Ward A. K., 2004, The Messenger, 117, 27
Gehrels N., 1986, ApJ, 303, 336
Hambly N. C. et al., 2008, MNRAS, 384, 637
Hewett P. C., Warren S. J., Leggett S. K., Hodgkin S. T., 2006, MNRAS, 367, 454
Hodgkin S. T., Irwin M. J., Hewett P. C., Warren S. J., 2009, MNRAS, 394, 675
Irwin M. J. et al., 2004, in Quinn P. J., Bridger A., eds, Proc. SPIE, Vol. 5493, Optimizing Scientific Return for Astronomy through Information Technologies. SPIE, Bellingham, p. 411
Kroupa P., 2002, Sci, 295, 82
Kroupa P., Weidner C., Pflamm-Altenburg J., Thies I., Dabringhausen J., Marks M., Maschberger T., 2011, preprint (arXiv:1112.3340)
Kunkel M., 1999, PhD thesis, Julius-Maximilians-Universität Würzburg
Lawrence A. et al., 2007, MNRAS, 379, 1599
Lodieu N., Hambly N. C., Jameson R. F., 2006, MNRAS, 373, 95
Lodieu N., Hambly N. C., Jameson R. F., Hodgkin S. T., Carraro G., Kendall T. R., 2007, MNRAS, 374, 372
Lodieu N., Hambly N. C., Jameson R. F., Hodgkin S. T., 2008, MNRAS, 383, 1385
Lodieu N., Zapatero Osorio M. R., Rebolo R., Martín E. L., Hambly N. C., 2009, A&A, 505, 1115
Lodieu N., Hambly N. C., Dobbie P. D., Cross N. J. G., Christensen L., Martin E. L., Valdivielso L., 2011a, MNRAS, 418, 2604
Lodieu N., Dobbie P. D., Hambly N. C., 2011b, A&A, 527, A24
Lodieu N., Deacon N. R., Hambly N. C., Boudreault S., 2012a, MNRAS, 426, 3403
Lodieu N., Deacon N. R., Hambly N. C., 2012b, MNRAS, 422, 1495
Lodieu N., Ivanov V. D., Dobbie P. D., 2013, MNRAS, 430, 1784
Luhman K. L., Mamajek E. E., 2012, ApJ, 758, 31
Luhman K. L. et al., 2005, ApJ, 631, L69
Martín E. L., Delfosse X., Guieu S., 2004, AJ, 127, 449
Martín E. L. et al., 2010, A&A, 517, A53
Miller G. E., Scalo J. M., 1979, ApJS, 41, 513
Pecaut M. J., Mamajek E. E., Bubar E. J., 2012, ApJ, 746, 154
Peña Ramírez K., Béjar V. J. S., Zapatero Osorio M. R., Petr-Gotzens M. G., Martín E. L., 2012, ApJ, 754, 30
Preibisch T., Zinnecker H., 1999, AJ, 117, 2381
Preibisch T., Zinnecker H., 2002, AJ, 123, 1613
Preibisch T., Guenther E., Zinnecker H., Sterzik M., Frink S., Roeser S., 1998, A&A, 333, 619
Preibisch T., Guenther E., Zinnecker H., 2001, AJ, 121, 1040
Riaz B., Lodieu N., Gizis J. E., 2009, ApJ, 705, 1173
Riaz B., Lodieu N., Goodwin S., Stamatellos D., Thompson M., 2012, MNRAS, 420, 2497
Salpeter E. E., 1955, ApJ, 121, 161
Scalo J. M., 1986, Fundam. Cosm. Phys., 11, 1
Scholz A., Jayawardhana R., Wood K., Meeus G., Stelzer B., Walker C., O'Sullivan M., 2007, ApJ, 660, 1517
Scholz A., Xu X., Jayawardhana R., Wood K., Eislöffel J., Quinn C., 2009, MNRAS, 398, 873
Slesnick C. L., Carpenter J. M., Hillenbrand L. A., 2006, AJ, 131, 3016
Slesnick C. L., Hillenbrand L. A., Carpenter J. M., 2008, ApJ, 688, 377
Song I., Zuckerman B., Bessell M. S., 2012, AJ, 144, 8
van Leeuwen F., 2009, A&A, 497, 209
Walter F. M., Vrba F. J., Mathieu R. D., Brown A., Myers P. C., 1994, AJ, 107, 692
Wright E. L. et al., 2010, AJ, 140, 1868

APPENDIX A: USCO MEMBER CANDIDATES IN THE *ZYJHK* – PM REGION FREE OF REDDENING

Table A1. Sample of 201 USco member candidates in the GCS DR10 PM region devoid of reddening, including known members previously published in the literature. This table is available electronically in the online version of the journal.

RA	Dec.	$Z \pm$ err	$Y \pm$ err	$J \pm$ err	$H \pm$ err	$K1 \pm$ err	$K2 \pm$ err	$\mu_\alpha \cos\delta \pm$ err	$\mu_\delta \pm$ err	χ^2
15:41:26.54	−26:13:25.5	15.649 ± 0.005	14.788 ± 0.003	13.999 ± 0.003	13.406 ± 0.003	12.971 ± 0.002	12.986 ± 0.002	−7.31 ± 2.70	−17.66 ± 2.70	0.58
15:41:54.34	−25:12:43.6	15.588 ± 0.005	99.999 ± 99.999	14.435 ± 0.004	13.729 ± 0.003	13.422 ± 0.003	13.457 ± 0.003	−8.05 ± 1.97	−24.10 ± 1.97	4.28
...	...	...	...	...	...	...	...	...	...	...
16:37:05.23	−26:25:44.2	14.266 ± 0.003	13.605 ± 0.002	12.963 ± 0.002	12.461 ± 0.002	12.082 ± 0.001	12.088 ± 0.001	−7.65 ± 2.69	−20.81 ± 2.69	0.68
16:37:54.43	−26:51:52.0	12.968 ± 0.001	12.507 ± 0.001	11.923 ± 0.001	11.459 ± 0.001	11.096 ± 0.001	11.142 ± 0.001	−6.53 ± 2.69	−22.52 ± 2.69	0.84

APPENDIX B: USCO MEMBER CANDIDATES IN THE *ZYJHK* – PM REGION AFFECTED BY REDDENING

Table B1. Sample of 120 USco member candidates in the GCS DR10 PM region affected by reddening, including known members previously published in the literature. This table is available electronically in the online version of the journal.

RA	Dec.	$Z \pm$ err	$Y \pm$ err	$J \pm$ err	$H \pm$ err	$K1 \pm$ err	$K2 \pm$ err	$\mu_\alpha \cos\delta \pm$ err	$\mu_\delta \pm$ err	χ^2
16:16:20.73	−25:17:30.1	13.316 ± 0.002	12.800 ± 0.001	12.192 ± 0.001	11.528 ± 0.001	11.171 ± 0.001	11.231 ± 0.001	−4.56 ± 1.82	−16.57 ± 1.82	0.53
16:16:30.68	−25:12:20.3	14.208 ± 0.003	13.549 ± 0.002	12.887 ± 0.001	12.320 ± 0.002	11.935 ± 0.001	11.936 ± 0.001	−12.30 ± 1.82	−19.96 ± 1.82	0.48
...	...	...	...	...	...	...	...	...	...	...
16:39:49.31	−24:33:10.1	14.232 ± 0.003	13.771 ± 0.002	13.169 ± 0.002	12.501 ± 0.001	12.267 ± 0.001	12.266 ± 0.001	−12.25 ± 1.83	−21.05 ± 1.83	0.54
16:40:47.51	−24:04:38.9	19.594 ± 0.069	18.269 ± 0.030	17.073 ± 0.022	15.881 ± 0.014	15.364 ± 0.015	15.334 ± 0.010	−7.17 ± 2.38	−17.62 ± 2.38	8.88

APPENDIX C: USCO MEMBER CANDIDATES IN THE GCS SV

Table C1. Sample of 81 USco member candidates identified in the GCS SV area, including previously known members. The proper motion measurements come from the 2MASS/GCS cross-match. This table is available electronically in the online version of the journal.

RA	Dec.	$Z \pm$ err	$Y \pm$ err	$J \pm$ err	$H \pm$ err	$K1 \pm$ err	$\mu_\alpha \cos\delta$	μ_δ
16:06:03.75	−22:19:30.0	18.169 ± 0.036	16.825 ± 0.014	15.853 ± 0.009	15.096 ± 0.009	14.438 ± 0.009	13.67	−26.51
16:06:06.29	−23:35:13.3	18.430 ± 0.041	17.150 ± 0.018	16.204 ± 0.012	15.540 ± 0.012	14.973 ± 0.012	−6.08	5.64
...	...	...	...	...	...	...	...	...
16:17:01.47	−23:29:06.0	13.656 ± 0.002	13.025 ± 0.002	12.453 ± 0.001	11.887 ± 0.001	11.537 ± 0.001	−17.93	−19.58
16:17:06.06	−22:25:41.6	13.254 ± 0.002	12.663 ± 0.002	12.120 ± 0.001	11.516 ± 0.001	11.202 ± 0.001	−15.03	−26.36

APPENDIX D: USCO MEMBER CANDIDATES IN THE *HK* SAMPLE

Table D1. Sample of 286 USco member candidates identified in the USco region imaged in *H* and *K* only, including previously known members. This table is available electronically in the online version of the journal.

RA	Dec.	$H \pm$ err	$K \pm$ err	$\mu_\alpha \cos\delta$	μ_δ
15:40:10.22	−24:31:18.4	14.538 ± 0.004	13.818 ± 0.004	0.31	−9.96
15:41:16.03	−25:30:56.5	14.932 ± 0.008	14.305 ± 0.008	−9.04	−7.19
...	...	...	...	...	...
16:40:19.60	−22:18:12.0	13.361 ± 0.002	12.953 ± 0.002	0.36	−5.89
16:40:24.95	−22:18:52.8	12.871 ± 0.002	12.450 ± 0.002	5.38	−13.56

APPENDIX E: USCO MEMBER CANDIDATES WITH WISE PHOTOMETRY

Table E1. Sample of 660 USco member candidates identified in GCS DR10 with *WISE* photometry, ordered by increasing right ascension. The coordinates are from the UKIDSS GCS DR10 data base whereas the photometry is from the *WISE* all-sky release. Objects detected in two, three and four *WISE* bands are marked as 1100, 1110 and 1111 (column 7; wise_detect), respectively. This table is available electronically in the online version of the journal.

RA	Dec.	$w1 \pm$ err	$w2 \pm$ err	$w3 \pm$ err	$w4 \pm$ err	wise_detect
15:40:10.22	−24:31:18.4	13.733 ± 0.031	13.829 ± 0.048	12.462 ± 0.000	8.811 ± 0.000	1100
15:41:16.03	−25:30:56.5	14.226 ± 0.034	14.330 ± 0.079	12.185 ± 0.000	8.764 ± 0.000	1100
...	...	...	...	...	...	...
16:40:24.95	−22:18:52.8	12.113 ± 0.024	12.012 ± 0.028	11.473 ± 0.278	7.397 ± 0.117	1100
16:40:47.51	−24:04:38.9	15.028 ± 0.054	14.773 ± 0.093	11.426 ± 0.000	8.249 ± 0.000	1100

SUPPORTING INFORMATION

Additional Supporting Information may be found in the online version of this article:

Table A1. Sample of 201 USco member candidates in the GCS DR10 PM region devoid of reddening, including known members previously published in the literature.
Table B1. Sample of 120 USco member candidates in the GCS DR10 PM region affected by reddening, including known members previously published in the literature.
Table C1. Sample of 81 USco member candidates identified in the GCS SV area, including previously known members.
Table D1. Sample of 286 USco member candidates identified in the USco region imaged in *H* and *K* only, including previously known members. This table is available electronically in the online version of the journal.
Table E1. Sample of 660 USco member candidates identified in GCS DR10 with *WISE* photometry, ordered by increasing right ascension. (http://mnras.oxfordjournals.org/lookup/supp1/doi:10.1093/mnras/stt402/-/DC1)

Please note: Oxford University Press are not responsible for the content or functionality of any supporting materials supplied by the authors. Any queries (other than missing material) should be directed to the corresponding author for the article.

This paper has been typeset from a TEX/LATEX file prepared by the author.